Tribology and hot forming performance of self-lubricious NC/NiBN and NC/WC:C hybrid composite coatings for hot forming die

Dong, Yangchun; Zheng, Kailun; Fernandez, Jonathan; Fuentes, Gonzalo; Li, Xiaoying; Dong, Hanshan

DOI:
10.1016/j.jmatprotec.2017.09.025

Document Version
Peer reviewed version

Citation for published version (Harvard):
Dong, Y, Zheng, K, Fernandez, J, Fuentes, G, Li, X & Dong, H 2018, 'Tribology and hot forming performance of self-lubricious NC/NiBN and NC/WC:C hybrid composite coatings for hot forming die', *Journal of Materials Processing Technology*, vol. 252, pp. 183-190. https://doi.org/10.1016/j.jmatprotec.2017.09.025

Title: Tribology and hot forming performance of self-lubricious NC/NiBN and NC/WC:C hybrid composite coatings for hot forming die

Authors: Yangchun Dong, Kailun Zheng, Jonathan Fernandez, Gonzalo Fuentes, Xiaoying Li, Hanshan Dong

PII: S0924-0136(17)30424-7
DOI: http://dx.doi.org/10.1016/j.jmatprotec.2017.09.025
Reference: PROTEC 15402

To appear in: *Journal of Materials Processing Technology*

Received date: 29-6-2017
Revised date: 11-9-2017
Accepted date: 15-9-2017

Please cite this article as: Dong, Yangchun, Zheng, Kailun, Fernandez, Jonathan, Fuentes, Gonzalo, Li, Xiaoying, Dong, Hanshan, Tribology and hot forming performance of self-lubricious NC/NiBN and NC/WC:C hybrid composite coatings for hot forming die.Journal of Materials Processing Technology http://dx.doi.org/10.1016/j.jmatprotec.2017.09.025

Tribology and hot forming performance of self-lubricious NC/NiBN and NC/WC:C hybrid composite coatings for hot forming die

Yangchun Dong[1,a], Kailun Zheng[2], Jonathan Fernandez[3], Gonzalo Fuentes[3], Xiaoying Li[1], Hanshan Dong[1]

[1] School of Metallurgy and Materials, University of Birmingham, B15 2TT Birmingham, UK

[2] Department of Mechanical Engineering, Imperial College London, SW7 2AZ London, UK

[3] AIN Asociación de la Industria Navarra, 31191 Navarre, Spain

Graphical abstract

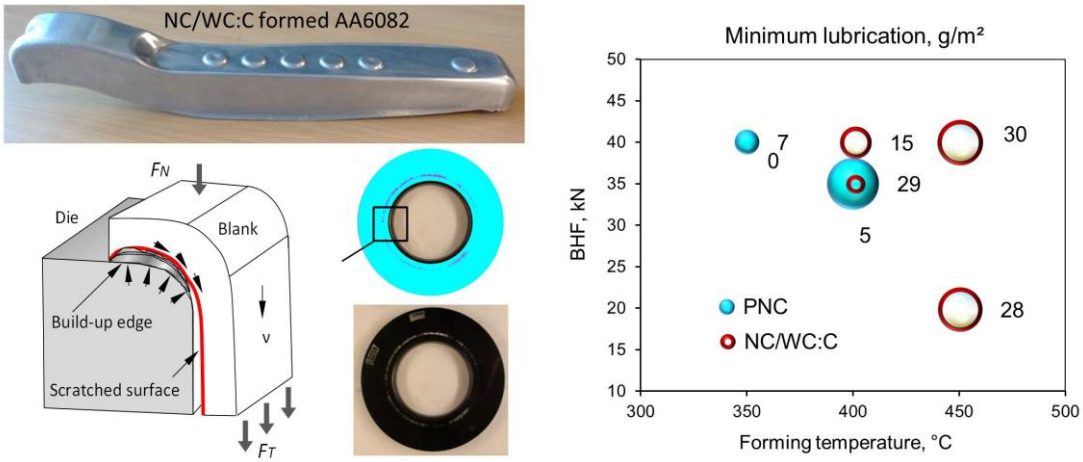

Abstract: Adhesion between blank and die is the main reason for seizure and short tooling life during metal forming processes at elevated temperatures. This study applied novel complex-structured composite coatings, NC/NiBN and NC/WC:C, to the hot forming die flange and radius to reduce the use of lubricant. The high-temperature adhesion resistance and hot forming properties of the hybrid coated dies were tested and correlated with the microstructure and mechanical properties of the

[a] Corresponding author

contacted blank/tool surfaces. The results show that the coated dies experienced little adhesion at elevated temperatures, consequently, ultra-low coefficients of friction of 0.11 against steel and 0.10 against Al at 350 °C were obtained. The minimum weight of lubricant per unit area required for a successful deep drawing of AA6082 was quantified by hot forming tests at various temperatures, and it was reduced by 83% at 400 °C. Complete lubricant-free deep drawing was achieved with limited blankholding force and forming temperature. Based on this experimental data and theoretical analysis of two disparate stress states, a model comparing the frictional state of material surfaces using the geometric features on formed parts is proposed.

Keywords: Tool coating, Dry machining, Adhesion, Aluminium alloy

1 Introduction[b]

Hot stamping of lightweight high-strength materials such as aluminium alloys for the manufacture of panel components is an effective technology for reducing gas emissions in the automotive industry (Mohamed et al., 2012). In order to overcome the poor ductility of aluminium and magnesium alloys, a novel hot stamping process, named "Solution Heat treatment, cold die Forming and Quenching (HFQ®)" patented by Lin et al. (2008), allows the mass-production of complex-shaped high strength aluminium alloy components. During HFQ® forming, the initial blank is solution heat treated to

---

[b] Abbreviations

ASPN active screen plasma nitriding
ASPNC active screen plasma nitrocarburising
BHF blankholding force
CoF coefficient of friction
CoF_M mean coefficient of friction
DLC diamond-Like carbon
EDS energy dispersive spectroscopy
FIB focused ion beam
HFQ® solution heat treatment, cold die forming and quenching
NiBN boron nitride doped nickel
PN plasma nitriding
PNC plasma nitrocarburising
PVD physical vapour deposition
SEM scanning electron microscope
SD standard deviations
WC:C tungsten doped carbon

dissolve the original precipitates, and then quickly transferred to the cold dies, formed and in-die quenched to low temperatures. Zheng et al. (2017) numerically determined the complex distribution of temperature on die flanges and corners of different textured drawing dies, and proposed that in comparison with conventional cold stamping process, stamping dies used for the hot stamping aluminium alloys face stringent requirements. They are: (1) low friction at elevated temperatures; (2) wear-resistant particularly against the soft and chemically reactive aluminium alloys; (3) good in-die quenching performance. To this end, high-temperature lubricant is indispensable to meet these requirements. However, pre-brushing and post-cleaning of lubricant increased the processing time and the total manufacturing cost.

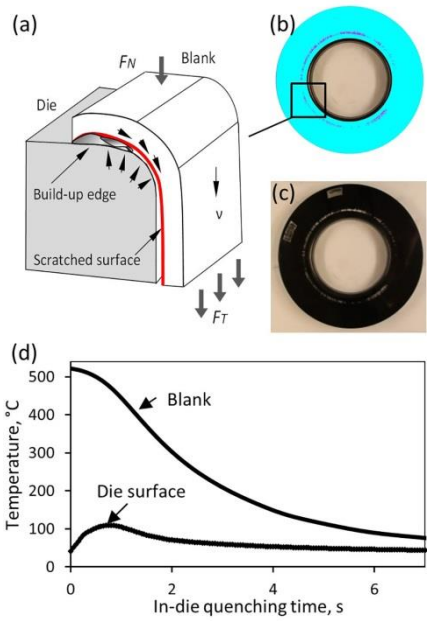

Fig. 1. (a) Illustration of material adhesion between blank and forming die, (b) extracted adhesion area in purple and (c) top view of a used die showing aluminium adhesion area near the built-up edge (d) measured temperatures of blank and die surfaces during HFQ® cup forming.

Environmentally friendly lubricant-free or near-lubricant-free forming is attractive to the large volume mass-production. However, a review by Karbasian and Tekkaya (2010) pointed out that it is

challenging to reduce the usage of lubricant because of the risk of severe adhesive wear during the dry stamping process. Diffusion of metal elements from the stressed blank to the die surface affects not only the tool service life, but equally importantly the metal flow behaviours of sheet materials. Fig. 1 illustrates the die/blank geometry and temperature variations during an HFQ® process. During hot stamping, the most severe tool failures, such as wear and galling, are experienced often in the flange area due to the high temperature and high-stress working conditions. Excessive friction in the flange area may constrain material flow and result in tearing at the die entrance and over-thinning of the side wall areas.

Since the adhesive wear takes place at the blank/tool interface, some adaptive lubricious coatings were deposited on the tool surface to address this problem. Diamond-like carbon (DLC) and nano-C thin films deposited using PVD or plasma deposition technologies are the most studied anti-adhesive coating systems for machining tools. Carlsson and Olsson (2006) have investigated the anti-galling properties of DLC coating sliding against Zn-coated steel, and found that it exhibited excellent protection against the material pick-up. Murakawa and Takeuchi (2003) applied DLC to the aluminium forming and confirmed the reducing of aluminium adhesion during forming and the reduction of coefficient of friction (CoF) to 0.2. The applications of DLC coatings have been extended to many machining processes, such as drilling (Bhowmick and Alpas, 2008) and cutting (Fukui et al., 2004), all of which involve testing aluminium adhesion under high-stress sliding contact. Hence, these results are good references for the evaluation of tooling performance in this study.

In spite of excellent properties of DLC coated surfaces at room temperature, DLC coating has a poor tribological performance at temperatures above 300 °C, which inhibited their applications for the hot stamping conditions. Dong et al. (2017) found that dry forming of Al-Mg-Si sheet using the DLC coated top-hat part drawing tools become susceptible to adhesion on the die radius at 350 °C. Therefore, in this study, a coating system ingrained with elements that have phase transformations

to lubricious oxides at elevated temperatures, such as tungsten (W), was applied rather than searching for a thermally stable coating. In addition, Dong et al. (2015) found that the loading capacity of a coating can be increased by inserting a strong underlayer, such as nitrocarburising (NC) case, between the coating and substrate.

In this research, a hybrid composite coating system NC/X were designed for hot forming dies by combining a lubricious composite top coating (X) with a nitrocarburised deep case via plasma nitrocarburising , aiming for the maximised mechanical support and lubricity at high temperatures. The hot forming performance of NC/X coated dies was assessed using a deep-drawn top-hat apparatus under the HFQ® conditions. The frictional properties of NC/X hybrid coating against steels and aluminium at elevated temperatures were comprehensively analysed, and the mechanism of solid lubricity at the coating/blank interface was explored.

2 Material and method

2.1 Tooling materials and coating technologies

Gray cast iron (automotive metric standard NAAMS G3500 with nominal composition (wt%, 3.2 C, 1.2 Si, 0.5 Mn, 0.5 Cr, 0.5Mo, balance Fe) was selected as the die material due to its excellent mechanical and thermal properties. Deep drawing tools and test pieces were cast and then stress relieved at 690 °C for 2 h, followed by machining, polishing and acetone cleaning prior to treatments. To synthesis NC/X composite coating, the two-step surface treatment processes were used sequentially: a) active screen plasma nitriding (ASPN) or nitrocarburising (ASPNC) cast iron to produce underlayer, followed by b) a carbon or nickel based non-stick composite coating as the overlayer. Therefore, the samples can be divided into four groups according to the applied surface treatments, with the sample codes, treatment temperature *T* and time *t* of each step summarised in Table 1.

ASPNC was conducted in an industrial scale active screen plasma furnace (Klöckner 40 kW, Germany). The setup of ASPNC process can be found in (Dong et al., 2011). The following treatment conditions were applied: source electrode voltage of 1200 V, substrate voltage of 300 V, 5% bias on the work table, gas mixture of 50% H_2 + 48% N_2 + 2% CH_4, 4 mbar working pressure and 4 h treatment duration. In comparison, ASPN was carried out at 525 °C, 24 h with 75% H_2 and 25% N_2. Cleaned by the glow discharge plasma during underlayer treatment, cast iron was subsequently deposited with the following overlayer. Boron nitride doped nickel (NiBN) coating was prepared using electroless nickel plating, in a bath mixture of 5 vol% Ni component, 15 vol% chelate-reducer and 100 g/L hBN dispersion. The tungsten doped carbon (WC:C) coating was synthesised by means of cathodic arc enhanced PVD at 200-350 °C. Embedded tungsten was controlled to be amorphous (non-crystallites), targeting the most substantial decrease of adhesion and friction coefficient.

Table 1. Conditions of tooling surface treatments

		PNC	PN	NC/NiBN	NC/WC:C
Overlayer	Process	-	-	Ni-BN plating	PVD WC:C
	T, °C			88	350
	t, h			1	1.5
Underlayer	Process	ASPNC	ASPN	ASPNC	ASPNC
	T, °C	575	525	575	575
	t, h	4	24	4	4

2.2 High-temperature adhesion test

A pin-on-disk circular track tribometer (CSM HT Tribometer) was used to assess the metallic transfer at the coating/tool interface at various temperatures (standard ASTM G99). Billur (2010) proposed that either pin-on-disc or forming trails can be used for the evaluation of tribology properties of tools. In this study, both methods were used to evaluate the tribological performance of the coated tools. Pin-on-disc test recorded the CoF and the initiating of adhesion in real-time; forming trials

validated the hypothesized performance of selected tools on various forming parameters. The detailed set-up of the adhesion test on pin-on-disc was given by Dong et al. (2017). A coated disc was firstly heated to target temperature and the aluminium pin was heated through direct contact with the coated tools for 15 mins before the test. Untreated G3500, PN, PNC and NC/X coated specimens were tested under simulated forming temperatures from 20°C to 450°C, under a Hertzian contact pressure of 481 MPa: 200 gf, for 500 cycles. The mechanism of adhesion was analysed on different blank materials: hardened steel (100Cr6) and AA 6082-O pins. A new pin was used for each test and three repeated tests were carried out in random areas.

2.3 Hot stamping trials

The sheet material selected for the top-hat drawing test was the commercial AA6082-T6 (Smiths Metal Centres, UK). The chemical composition of AA6082 is given in Table 2. Aluminium alloy sheet with the thickness of 1.5 mm was laser cut to a circular shape with a diameter of 170 mm. The test piece was then solution heat treated at 535 °C for 2 mins and hot formed at 350 °C, 400 °C and 450 °C with various blankholding force (BHF).

Table 2. Material composition of AA6082 sheet

Element	Si	Mg	Mn	Zn	Cu	Ti	Cr	Fe	Al
wt %	0.7-1.3	0.6-1.2	0.4-1.0	<0.2	<0.1	<0.1	<0.25	<0.5	Balance

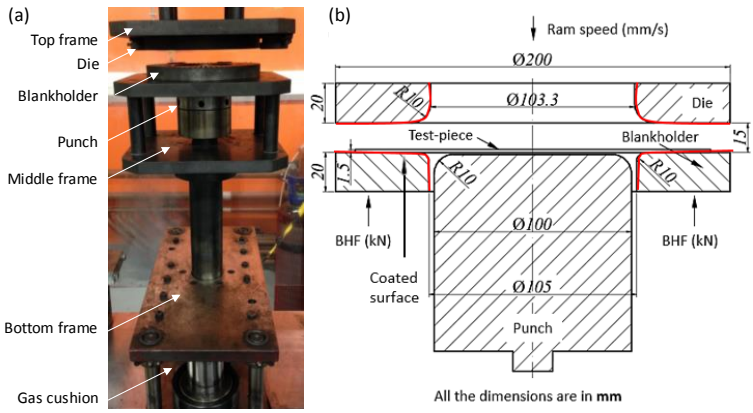

Fig. 2. Materials and experimental set-up of hot forming: (a) deep drawing test-rig and (b) geometry and dimensions of tools.

A cylindrical deep drawing test was utilised to assess the lubrication performances of treated tool surfaces under the HFQ® conditions. The emphasis of this study was to validate the formability and the frictional states of tools, and quantify the minimum amount of required lubricant. Fig. 2 shows the deep drawing test rig, the geometry and dimensions of die, punch and blankholder (Zheng et al., 2017). The corresponding drawing ratio ($D_R = D_{blank}/D_{punch}$) was 1.7, where D_{blank} and D_{punch} represent blank and punch diameter respectively. A graphite-based water-soluble lubricant was applied between the blank/tool interface and the applied weight was precisely measured to 0.01 g by a digital balance. The minimum amount of lubricant was tested using the method of conceptual binary search. The reference amount of lubricant at fully lubricated condition is divided into several search spaces, and for each trial, it halves the search space until after at most 4 steps the approximate match of minimum lubricant range is obtained. Then, the upper value in this range is reported due to a limited number of trials the experiments can implement. Finally, the value of lubrication condition on the duplex surface treated tool surface was reflected by the surface lubricant density defined in Eq. (1).

$$D_l = m_l/A \tag{1}$$

Where m_l represents the weight of used lubricant, and A represents the lubricant applied area (199 cm^2) between test-piece material and surface treated tool.

2.4 Confocal topography and interface analysis

In order to analyse the mechanism of adhesion at the blank/tool interface, the morphology and chemical composition of coated tool before and after adhesion test were analysed by a field-

emission scanning electron microscope (SEM, JEOL 7000), equipped with an energy dispersive spectroscopy (EDS, Oxford Instrument). Three-dimensional post-test topography was measured in the contact area using a confocal optical microscopy (Olympus Lext OLS300). In addition, the mechanical properties of tooling and blank materials before and after adhesion tests were carried out on the polished samples using a nanoindentation (Micro Materials Ltd). The nanoindentation measurement was performed in the load-control mode with a maximum load of 50 mN at a constant loading/unloading speed of 0.5 mN/s. Ten indentations were performed to verify the accuracy and scatter of the indentation data. In addition, a site-specific sample extracted for microanalysis inside the adhesion area was prepared using a dual beam FEI Quanta 3D FEG focused ion beam (FIB) technique, which cut to the accuracy of sub-micrometres by the focused Ga^+ irons. A 30 x 3 µm surface of the wear track was firstly coated with 3 µm Pt coating to prevent contamination, and then ion beam milled perpendicular to the sliding direction of the wear track at 65 nA (trenching), 30 nA (micromachining) and 1 nA (polishing). In-situ observation of the cross-sectional area was performed by SEM and the elemental concentration at the interface of adhesion was measured by EDS.

3 Results

3.1 Tool coating microstructure

The top views of the NC/NiBN and NC/WC:C coated tools are shown in Fig. 3a, 3b. SEM images showed that the NC/NiBN overlayer is smooth and has some embedded BN particles exposure on the top surface. NC/WC:C coating, on the other hand, shows a top view of the uniform columnar microstructure. The transverse cross-section morphologies and composition of NC/X hybrid coating are shown in Fig. 3c-3f. All NC/X coatings are composed of a PNC underlayer, a plasma cleaned oxygen-free interface (OFI) and a functional composite overlayer of NiBN or WC:C. Dong (2010) reported that iron oxides pre-existed on the cast iron surface were removed by the plasma during

the first step, resulting in a clean PNC surface that is not susceptible to the moisture in the atmosphere. This is known as the OFI, by which the bonding strength to the subsequent overlayer can be enhanced.

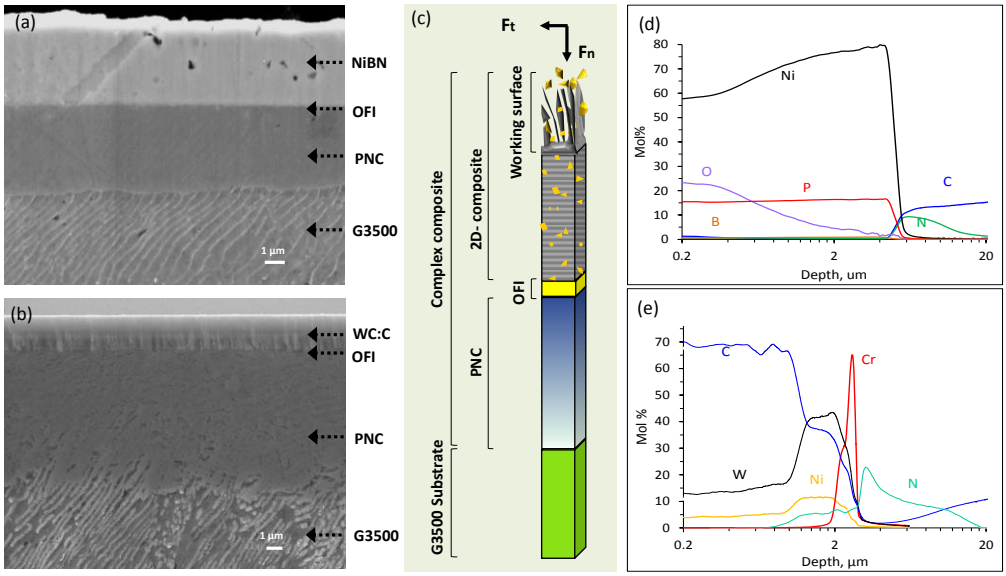

Fig. 3. Transverse cross-section of NC/X coating system showing (a, b) SEM top view of NC/NiBN and NC/WC:C, respectively; (c, d) corresponding cross-sectional structures; (e, f) GDOES chemical composition profiles from the surface to the substrate of NC/NiBN and NC/WC:C, respectively.

A close observation of the cross-sectional microstructures Fig. 3a and 3b show that NC/NiBN and NC/WC:C, having the total thickness of approximately 15 and 12.5 µm, respectively, were deposited on the tooling surface. For Ni/BN, BN particles embedded in the Ni-P matrix are visible in Fig. 3c. In contrast, WC:C overlayer has a columnar structure with the decreasing columnar size towards the surface. GDOES results showed that the composition of the NiBN overlayer is $Ni_{0.65}P_{0.16}O_{0.18}(BN)_{0.01}$, whereas the WC:C is $W_{0.18}C_{0.7}Ni_5$. The underlayer ranging from 3 µm to 15 µm in depth is rich in N, and the long-tail line of gradually decreasing N in this layer is the result of interstitial diffusion of N in cast iron.

3.2 Aluminium adhesion test

3.2.1 Effect of tooling surface treatment

The CoF trend of G3500, PN/PNC and NC/X coated tools sliding against dry aluminium pins are displayed in Fig. 4. Pearson-correlation analysis shows there is no significant dependence of CoF on the number of cycles (p>0.01), although the CoF fluctuated markedly during the 500 cycles as evidenced in their large standard deviations (SD). The maximum CoF of untreated G3500 was 0.72 at 230th cycle and it increased to 0.92 for PNC and 0.82 for PN. It is believed that the fluctuation of CoF was triggered by the adhesion between two sliding surfaces–a zone of severely deformed soft metal that tenaciously adhere on and removed from the contact surface. Likewise, the great variations of CoF resulting from the persistent issue of adhesion on PNC and PN surfaces are still evident. In contrast, the coated tools (NC/NiBN and NC/WC:C) showed stable CoF throughout the 500 cycles. As shown in Fig. 4c, the CoF of Ni-BN quickly dropped to 0.60 at the very start and it maintained at around 0.65 for the rest of 500 sliding cycles, whereas NC/WC:C persisted mainly at the level of 0.02, but periodically increased to an upper range of 0.15. When the mean value of CoF (CoF_M) was considered for each test condition, the lowest CoF_M against aluminium can be found on the NC/WC:C tools, of which a significant depletion of CoF_M from 0.60 to 0.06 was obtained.

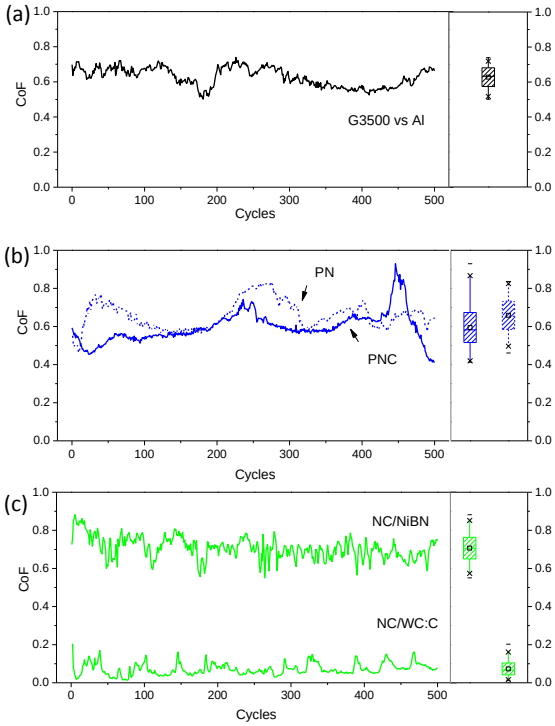

Fig. 4. CoF of (a) G3500, (b) PN and PNC, (c) NC/NiBN and NC/WC:C against Al at 350 °C, and their corresponding box plots with the 1st quartiles (box) and 1st standard deviations (whiskers) on the right cells.

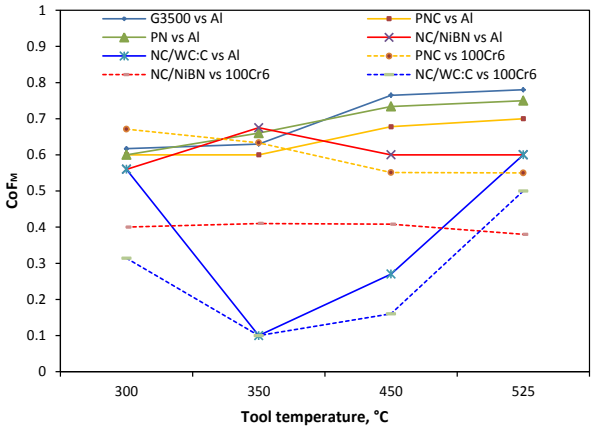

Fig. 5. Comparison of CoF_M ±SD of untreated and treated materials at various temperatures.

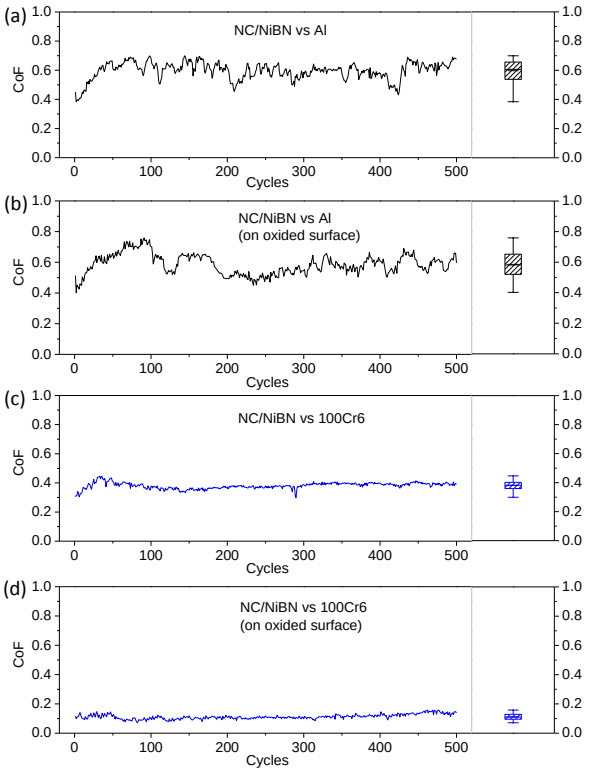

Fig. 6. Comparison of CoF of (a) NC/NiBN v.s. Al, (b) pre-oxidised NC/NiBN v.s. Al, (c) v.s. steel 100Cr6, and (d) pre-oxidised NC/NiBN v.s. steel 100Cr6. All tests were carried out at 525 °C.

3.2.2 Effect of temperature and forming material

Fig. 5 shows the evolution of CoF_M with the increasing temperature on various tooling materials. When the aluminium alloy was used as the pin, the CoF_M of untreated G3500, PNC and PN steadily increased with the increasing temperature from 300°C to 525°C, however, decreased at 450°C for NC/NiBN, and suddenly decreased to 0.10 at 350°C and then increased to 0.27 at 450°C for NC/WC:C. The effect of temperature on the CoF of coated tools was further analysed using counterpart of steel 100Cr6, as shown in Fig. 5. Compared to the aluminium results, it is interesting to see that the mean coefficient CoF_M decreased with the increasing temperature. This result is consistent with the results obtained from line/point contact sliding tests by Pearson et al. (2013) and Hutchings (1992), considering the increased ductility of steel at high temperatures. Therefore, sliding

with steel pin is dominated by the abrasion mechanism and it is different with the adhesion-prevalent mechanism for aluminium. The most interesting result can be seen on NC/NiBN, which exhibited diminution of CoF_M from 0.65 to 0.37. As exploited in Fig. 6, the 'NC/NiBN vs 100Cr6' shows that the CoF of NC/NiBN was comparatively smaller and less dispersed compared to sliding against aluminium (NC/NiBN vs Al). The standard deviation is halved from 0.1 to 0.05. This ultra-low CoF against steel was obviously relevant to the variation of chemical states at the coating/aluminium interface. Indeed, after pre-oxidising of the coating at 525°C, the CoF_M of NC/NiBN was further reduced to remarkably 0.11. By the end of 500 cycles, the CoF of NC/NiBN against steel was stable and smaller than the lowest CoF_M of NC/WC:C against steel.

3.3 Cylindrical deep drawing trial

Fig. 7a shows the featured 'zones' on a typical successfully HFQ® formed top-hat part relevant to the stress and deformation of materials during forming. The distance between the punch nose line and the remaining flange line marks the drawing depth of 45 mm. One important feature observed on the cup surface is that there exists a distinguish radius on the formed part, as shown in the line named sliding end (SE), where the section of surface above the SE line was smooth, whereas plenty of obvious mark and scratches existed on the surface of section below this line. In terms of flange material deformation in the deep drawing process, normally a two-dimensional contradict stress state was experienced, that is compressive stress, σ_r, in the hoop direction and tensile stress, σ_θ, in the radial direction. These two stresses can be calculated using Eq. (2) normally.

$$\begin{cases} \sigma_r = \sigma_f \ln\frac{r}{R_0} + \frac{2\mu P(R_0 - r)}{t} \\ \sigma_\theta = \sigma_f \left(\ln\frac{r}{R_0} - 1\right) + \frac{2\mu P(R_0 - r)}{t} \end{cases} \quad (2)$$

Where σ_f is the material flow stress, R_0 is the outer radius of flange, μ is the friction coefficient, P is the blankholding pressure, t is the test-piece thickness and r is the radius of infinitesimal small unit

in the flange. The outer edge flange material becomes thicker resulting from the compressive stress. However, the hoop stress changes from compressive to tensile with the position approaching to the inner edge of flange, according to Eq. (2) in (Marciniak et al., 2002). The limit position can be obtained when $\varepsilon_t = 0$, according to the Hooke's law in Eq. (3),

$$\varepsilon_t = \frac{\sigma_t}{E} - \frac{\nu}{E}(\sigma_r + \sigma_\theta) \tag{3}$$

Plane stress assumption is normally used for sheet stamping process. Then, stress in thickness direction assumes to be zero. The limit position can be obtained from Eq. (4) by substituting $\sigma_t = 0$ into Eqs. (2) and (3).

$$2lnr - Br = 1 - B + 2lnR_0 \tag{4}$$

Where B is expressed using Eq. (5)

$$B = \frac{2\mu P R_0}{\sigma_f t} \tag{5}$$

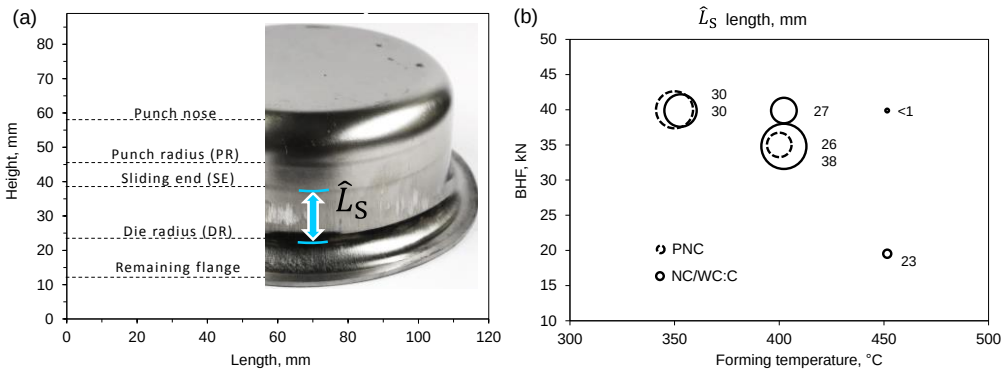

Fig. 7. (A) Geometry of an AA6082 top-hat part hot formed by a set of surface treated dies – note the SE line (b) measured $\hat{L}_S$ values on all the formed parts with the value indicated as the size of bubbles

As the position approaching the inner flange region, the material sustains a two-dimensional stress state, and the thickness of materials reduced. Meanwhile, the blank becomes thicker at the outer flange edge. With the CoF decreased in the coated flange area, the compressive stress becomes greater and radial tensile stress becomes smaller, the thickness transition point moves inwards and more material in the flange becomes thicker. Then, as the clearance between the punch and die is fixed, more material can be ironed and a distinctive line can be observed with the further drawing of flange material. It is discovered that the position of this line is correlated to the tooling friction status, i.e. the distance between the SE line and DR line (i.e. marked as $\hat{L}_s$) increased with the decreasing friction, thus $\hat{L}_s$ was used as an index of the latter.

Fig. 7b summarises the $\hat{L}_s$ values as the size of bubbles using the treated dies, at various forming temperatures and BHF. Due to the complexity of experimental design and manufacturing of tools, tools with the highest mechanical strength (PNC) and lowest CoF (NC/WC:C) were selected for trials. At 350 ℃, tribological behaviours of PNC and WC: C treated tools were similar — a 40 kN BHF contributed to a 30 mm $\hat{L}_s$. While at 400 ℃ and a 35 kN BHF, $\hat{L}_s$ of PNC decreased to 26 mm indicates a reduced performance of PNC tool under this forming condition. However, WC: C treated tools obtained a 38 mm $\hat{L}_s$ indicating that an improved frictional property of NC/WC:C treated dies which resulted in more flange material being deformed and drawn into the dies.

In addition, temperature is also an important process variable affecting the flange material deformation, thus it induces different $\hat{L}_s$. As can be seen in Fig. 7b, for WC: C treated tools, with the temperature increasing from 350 °C to 400 °C under a 40 kN BHF, the magnitude of $\hat{L}_s$ decreased from 30 mm to 27 mm. Moreover, the test-piece material cannot be drawn-in successfully with cracks formed around the die radius at 450 °C. The reason is that the blank becomes softer at the higher temperatures, till at a critical temperature, the flange friction surpass the material strength and the tear and crack happens. For hot stamping of aluminium alloys, the temperature distribution

of test-piece is non-uniform during the pressing due to the heat transfer between hot test-piece and cold dies; the temperature of die radius is higher than that of flange zone due to the less contact pressure with tools; on this region, the material strength is lower correspondingly. Hence, if the flange friction is too high, deformation may concentrate on this region resulting in tearing. On the contrary, the tools that exhibited a better tribological performance (i.e. NC/WC: C coating) would draw successfully at a higher temperature. For NC/WC:C coating, a successful drawn-in can be achieved at 450 °C by reducing the BHF to 20 kN ($\hat{L}_s$ =23 mm), while unachievable for PNC at such a condition.

The minimum weight of lubricant required by the untreated tools and NC/WC:C tools is summarised in Fig. 8. The forming speed was fixed at 300 mm/s. At 350 °C, the weight of lubricant for PNC was approximately 7 g/m^2. It can be reduced to zero (dry forming) using WC: C tools. When the temperature increased to 400 °C, a minimum amount of lubricant of 15 g/m^2 was needed for NC/WC:C tools, and the weight can be further reduced to 5 g/m^2 using a 35 kN BHF. This means that 83% less lubricant was needed to obtain a performance comparable to that of the fully lubricated tools. In addition, the minimum weight of lubricant required for a successful stamping of Al alloy increased with increasing temperature, which exhibits a similar behaviour to the increasing CoF with temperature in Fig. 5.

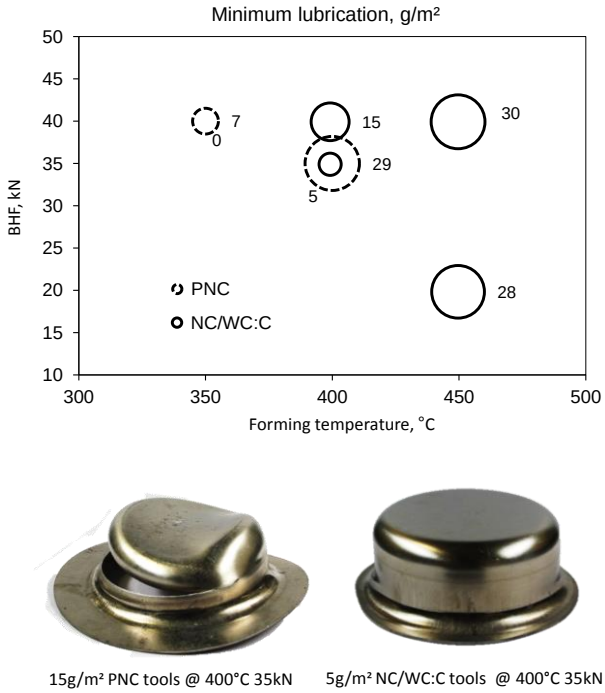

Fig. 8. The minimum amount of lubricant (g/m^2) required for a successful forming in the specified forming condition.

3.4 Adhesion interface analysis

After the hot forming tests, the microstructure of contact area on the tool surface was analysed by SEM as compared in Fig. 9. As for the untreated tool, the contact area is covered with a bright-coloured built-up area of Al film, particularly around the graphite edge. In comparison, no significant adhesion was found on NC/NiBN and NC/WC:C. The debris of Ni particles (confirmed by EDS) and some longitudinal grooves appeared on NC/NiBN along the graphite flakes after long-term exposure. The 3D profile of built-up area was analysed by the confocal laser 3D construction as shown in Fig. 10. It was discovered that up to 10 µm thick transfer layer can be seen on G3500 and PNC surfaces; as for the coated surfaces, plastic deformation and grooves of the coatings appeared, of which the deepest groove was 3 µm and 1.5 µm for NC/NiBN and NC/WC:C, respectively. In

summary, it is clear that the material transferred from Al pin to the tooling surface for G3500, PN and PNC. This explained the highly fluctuated CoF originated from continuous bonding, breaking and plastic deformation of the pin and substrate. Contrary to the fact that graphite is lubricious, the flake form of graphite acting like a cutting edge, in fact, is a preferred site for the adhesion. As for NC/NiBN and NC/WC:C, the low affinity between the two sliding surfaces contributes to the evidenced alteration of wear mechanisms, consequently, no Al was found on the EDS scan of the wear tracks (Fig. 10e-10f).

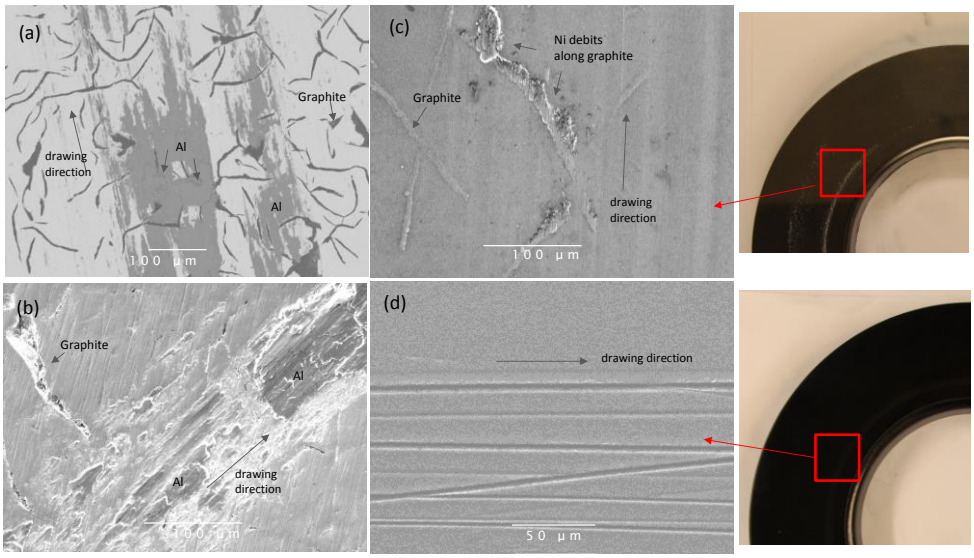

Fig. 9. SEM surface morphologies of the tool surfaces showing adhesion of aluminium on (a) G3500 and (b) PNC, (c) NC/NiBN and (d) NC/WC:C

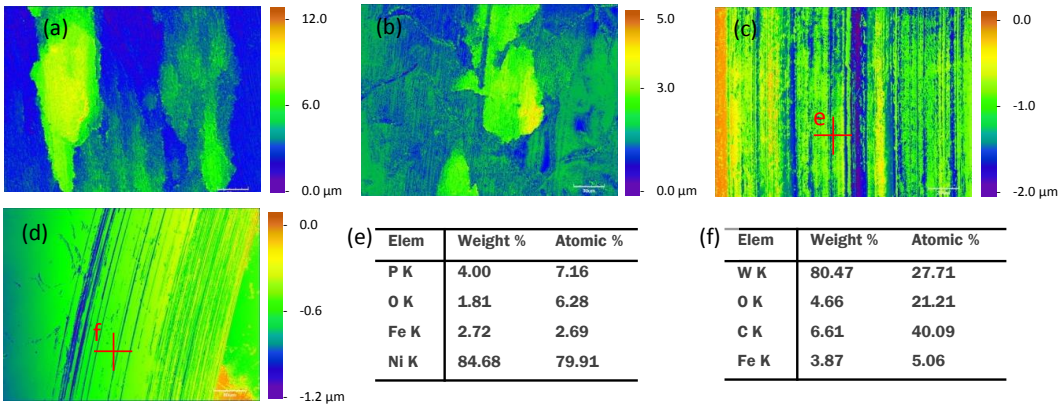

(e)

Elem	Weight %	Atomic %
P K	4.00	7.16
O K	1.81	6.28
Fe K	2.72	2.69
Ni K	84.68	79.91

(f)

Elem	Weight %	Atomic %
W K	80.47	27.71
O K	4.66	21.21
C K	6.61	40.09
Fe K	3.87	5.06

Fig. 10. Confocal microscope height mappings of (a) G3500, (b) PNC, (c) NC/Ni-BN, (d) NC/WC:C, v.s. Al (e, f) the EDS composition within the marked areas, condition: against Al, 350 °C.

However, despite the importance to reduce the adhesion for hot forming dies, the mechanism of adhesion inhibition is unknown for the produced NC/X functional coating. Considering it can be related to the mechanical properties of counterparts, the harnesses of Al alloy and tool surface before and after adhesion test were measured, as shown in Table 3. The post-test hardness H_{PW} is higher than the as-treated hardness H_{AT} hardness on the tooling surfaces, indicating the microstructure transformation of surface materials during the high-temperature adhesion test. The high content of oxygen found in the contact area is an evidence of oxidation (Fig. 10e-10f). According to the results of the cross-sectional FIB-SEM analysis in Fig. 11, nickel oxide was observed at the interface suggesting that the low friction property of the surface might be attributed to the formation of lubricious oxides. This is consistent with the fact that when sliding against steel, the CoF of NC/NiBN can be reduced by pre-oxidation (previously shown in Fig. 6). The crystallisation of NiBN after pin-on-disc test produces sharp Ni peaks and Ni_3P precipitate peaks, which can contribute to the very high H_{PW} of NC/NiBN at high temperatures. This reversal thermal-mechanical property of NC/NiBN (i.e. hardness increase with temperature) alters its frictional property (previously shown in Fig. 5) at a higher temperature. The FIB-SEM results indicated that the specified coating microstructure is required to enhance the tribological properties of tool coatings under the hot stamping conditions.

Table 3. Mechanical properties of the sliding counterparts

	As-treated H_{AT}, GPa	Post-test H_{PW}, GPa	E_r, GPa
AA6082	1.61 ± 0.22	1.63 ± 0.19	87± 4.21
G3500	3.66 ± 0.32	4.25 ± 0.33	172± 8.56

NC/WC: C	6.25 ± 0.50	7.00 ± 0.10	102± 5.20
NC/NiBN	6.35 ± 0.65	8.55 ± 0.30	154± 7.25
PNC	11.07 ± 0.42	11.93 ± 0.60	198± 10.01
PN	12.47 ± 0.48	12.50 ± 0.30	211± 11.10

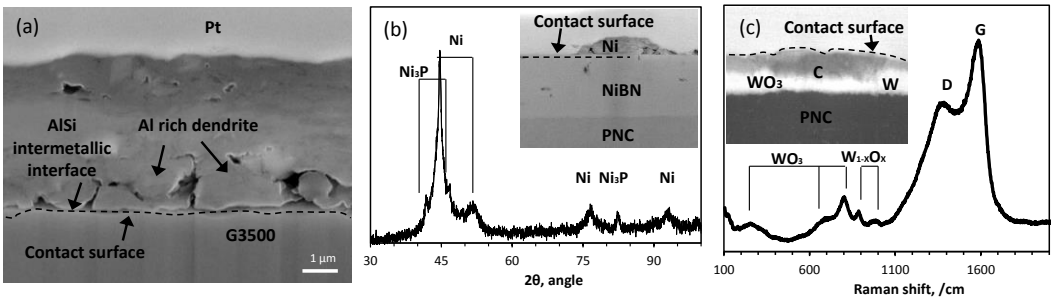

Fig. 11. Ion-induced secondary electron micrographs of FIB milled cross-sectional tool/blank interface on (a) G3500, (b) NC/NiBN with its XRD patterns, (c) NC/WC:C with its Raman spectrum inside the wear track, condition: against Al, 350 °C.

WC: C coating, on the other hand, might undergo a number of carbon phase transformations with the kinetic energy generated during sliding, from sp^2 to sp^3 carbon and to graphite. The EDS analysis showed half as much carbon in the wear debris after high-temperature wear tests suggesting the wear process is accompanied by consuming of C phase. Moreover, the transformation of amorphous WC to W_XC_{1-x} and W_XO_{1-x} crystalline as shown in Raman spectrum might also have an effect on the friction property. Gharam et al. (2011) previously found the W structure remains amorphous at low temperatures after wearing against aluminium, indicating the structural evolution is temperature-driven. Banerji et al. (2014) also observed the tungsten trioxide (WO_3) at high temperature sliding against Ti–6Al–4V. The role of above factors in altering the tribological property of aluminium stamping remains unclear. With the complex effect of carbon state and presenting of the self-lubricating possible Magnéli phases of tungsten oxides W_XO_{1-x} at elevated temperatures, further

studies needed to reveal the effect of microstructure evolution during environmental sliding of NC/NiBN and NC/WC:C coating. The detected low CoF of NC/WC:C against Al and NC/NiBN against steel evidence the fundamental difference between the intrinsic frictional characteristics of these two coatings. Above all, the analysis of wear scar morphology showed that the coating was not delaminated and it was bonded strongly with the substrate. This suggests a possible long service life of the soft-on-hard super-robust composite hybrid coating system.

4 Conclusions

A new type of composite coating NC/X was designed and applied to the hot forming dies using PVD and plasma nitrocarburising. The hybrid composite coating is composed of a newly developed hBN-embedded Ni coating or amorphous WC doped a-C coating as the overlayer and AS plasma NCed cast iron as the underlayer. The results of adhesion test and coefficient of friction analysis confirmed the initiating of adhesion from the graphite edges, which is the main reason for the metal transfer of Al onto the unlubricated grey cast iron dies. The oxides formed at elevated temperatures on the overlayers affected both the mechanical properties and contact mode at the tool/blank interface. The discovery of a sliding-end line on the surface of every hot formed cylinder has been theoretically explained and modelled linking to its in-situ frictional status. HFQ® forming trials have shown that NC/X composite coating is an efficient technique to prevent adhesion from the blank material and the NC/X coated tool requires less amount of hydro-lubrication to achieve competitive performance.

Acknowledgements

The authors gratefully acknowledge the financial support of the EU H2020 LoCoMaTech project [contract number GA723517]. Appreciation also is extended to the S.C. Plasmaterm S.A. Romania for the supply of raw materials; MacDermid Inc. UK for electroless plating service. The authors also thank Dr Daniel Reed for technical support of XRD, Raman and Confocal microscopy. HFQ® is a

registered trademark of Impression Technologies Ltd and HFQ® hot aluminium forming is a patented technology.

References

Banerji, A., Bhowmick, S., Alpas, A.T., 2014. High temperature tribological behavior of W containing diamond-like carbon (DLC) coating against titanium alloys. Surf. Coat. Tech. 241, 93-104. http://dx.doi.org/10.1016/j.surfcoat.2013.10.075

Bhowmick, S., Alpas, A.T., 2008. The performance of hydrogenated and non-hydrogenated diamond-like carbon tool coatings during the dry drilling of 319 Al. Int. J. Mach. Tools. Manuf. 48, 802-814. http://dx.doi.org/10.1016/j.ijmachtools.2007.12.006.

Billur, E., 2010. Continuing the look at die materials and wear in stamping AHSS Part II: Tests for evaluating galling, wear of tool materials and coatings. Stamping Journal.

Carlsson, P., Olsson, M., 2006. PVD coatings for sheet metal forming processes—a tribological evaluation. Surf. Coat. Technol. 200: 4654-4663. http://doi.org/10.1016/j.surfcoat.2004.10.127.

Dong, H., 2010. S-phase surface engineering of Fe-Cr, Co-Cr and Ni-Cr alloys. Int. Mater. Rev. 55, 65-98. http://dx.doi.org/10.1179/095066009X12572530170589

Dong, Y., Formosa, D., Fernandez, J., Li, X., Fuentes, G., Zoltan, K., Dong, H., 2015. Development of low-friction and wear-resistant surfaces for low-cost Al hot stamping tools. MATEC Web of Conferences, 21, 05009. http://dx.doi.org/10.1051/matecconf/20152105009

Dong, Y., Li, X., Tian, L., Bell, T., Sammons, R.L., Dong, H., 2011. Towards long-lasting antibacterial stainless steel surfaces by combining double glow plasma silvering with active screen plasma nitriding. Acta Biomater. 7, 447-457. https://doi.org/10.1016/j.actbio.2010.08.009

Dong, Y., Zheng, K., Fernandez, J., Li, X., Dong, H., Lin, J., 2017. Experimental investigations on hot forming of AA6082 using advanced plasma nitrocarburised and CAPVD WC: C coated tools. J. Mater. Process. Technol. 240, 190-199. http://dx.doi.org/10.1016/j.jmatprotec.2016.09.023.

Fukui, H., Okida, J., Omori, N., Moriguchi, H., Tsuda, K., 2004. Cutting performance of DLC coated tools in dry machining aluminum alloys. Surf. Coat. Technol. 187, 70-76. https://doi.org/10.1016/j.surfcoat.2004.01.014

Gharam, A.A., Lukitsch, M.J., Balogh, M.P., Irish, N., Alpas, A.T., 2011. High temperature tribological behavior of W-DLC against aluminum. Surf. Coat. Technol. 206, 1905-1912. http://dx.doi.org/10.1016/j.surfcoat.2011.08.002.

Hutchings, I.M., 1992. Tribology : friction and wear of engineering materials, second ed. Butterworth-Heinemann, Oxford.

Karbasian, H., Tekkaya, A.E., 2010. A review on hot stamping. J. Mater. Process. Technol. 210, 2103-2118. http://doi.org/10.1016/j.jmatprotec.2010.07.019.

Lin, J., Dean, T.A., Garrett, R.P., Foster, A.D., 2008. Process for forming metal alloy sheet components. Patent WO 2008059242 A2.

Marciniak, Z., Duncan, J.L., Hu, S.J., 2002. Cylindrical deep drawing. Mechanics of Sheet Metal Forming, second ed. Butterworth-Heinemann, Oxford, 117-128.

Murakawa, M., Takeuchi, S., 2003. Evaluation of tribological properties of DLC films used in sheet forming of aluminum sheet. Surf. Coat. Technol. 163–164, 561-565. DOI: http://dx.doi.org/10.1016/S0257-8972(02)00624-2.

Mohamed, M.S., Foster, A.D., Lin, J., Balint, D.S., Dean, T.A., 2012. Investigation of deformation and failure features in hot stamping of AA6082: Experimentation and modelling. Int. J. Mach. Tools. Manuf. 53(1), 27-38. https://doi.org/10.1016/j.ijmachtools.2011.07.005.

Pearson, S.R., Shipway, P.H., Abere, J.O., Hewitt, R.A.A., 2013. The effect of temperature on wear and friction of a high strength steel in fretting. Wear 303, 622-631. https://doi.org/10.1016/j.wear.2013.03.048.

Zheng, K., Lee, J., Lin, J., Dean, T.A., 2017. A buckling model for flange wrinkling in hot deep drawing aluminium alloys with macro-textured tool surfaces. Int. J. Mach. Tools. Manuf. 114, 21-34. https://doi.org/10.1016/j.ijmachtools.2016.12.008.